Textures and Microstructures, 1991, Vols 14–18, pp. 1239–1244
Reprints available from the publisher
Photocopying permitted by license only

TEXTURE EVOLUTION IN Zr-2.5 Nb DEFORMED IN UNIAXIAL COMPRESSION

A. SALINAS RODRIGUEZ AND J.H. ROOT
AECL Research, Chalk River, Ontario, K0J 1J0, CANADA

ABSTRACT

The evolution of texture in Zr-2.5 Nb during uniaxial compression was studied in annealed specimens with α grain sizes of 5 and 10 μm. It is shown that texture development is determined by the mechanism controlling <c>-axis deformation. In fine grained material <c+a> and <a> slip are found to be responsible for texture evolution. Tensile twinning controls the formation of a sharp [0001] compression texture in coarse grained material. It is suggested that the mode of <c>-axis deformation is determined by the α grain size.

INTRODUCTION

The texture of Zr-2.5 Nb CANDU pressure tubes can be described by a single $\{1\bar{2}10\}<10\bar{1}0>$ ideal orientation in which the (0001) plane normals of the crystal grains are aligned parallel to the circumferential direction. In 1982, it was discovered[1] that this texture leads to increased susceptibilities to delayed hydride cracking by promoting hydride reorientation in the presence of tensile circumferential stresses. Extensive research has been carried out at AECL to find alternative fabrication routes which may lead to pressure tubes with reduced cracking susceptibilities. The research to be described below forms part of this effort and was aimed at characterizing the evolution of texture in hot swaged Zr-2.5 Nb round bar during uniaxial compression.

EXPERIMENTAL

Zr-2.5 Nb bar stock, 12.7 mm in diameter, was employed as a starting material. The texture of the as-received bar consisted of a dual $[10\bar{1}0]$-[0001] fibre with the $[10\bar{1}0]$ component being predominant. Cylindrical specimens, 8 mm in diameter with an aspect ratio of 1.5, were machined to have their axial direction parallel to the axis of the bar. Two batches of specimens were vacuum annealed 24 hours at two different temperatures, 1073 K and 1123 K, and then furnace cooled. These produced microstructures consisting of equiaxed α-Zr grains with average grain sizes of 5 μm and 10 μm, respectively. Isolated regions of a second phase, presumably metastable bcc β-Zr, were also observed mainly at the corners of the α grains.

Compression testing was carried out at constant true strain rate of 5×10^{-4} s^{-1} in a computer controlled MTS-ALPHA system to true strains of up to -0.8. After deformation, texture was measured by neutron diffraction at the E-3 spectrometer located at the NRU research reactor. The wavelength of the incident beam was 1.398 Å and was obtained

from the (331) planes of a Si crystal monochromator at a diffraction angle of 68°. Intensity data were collected for the (0002), (10$\bar{1}$0), (11$\bar{2}$0), (10$\bar{1}$1) and (10$\bar{1}$2) reflections of α-Zr as a function of the tilt angle (0-90°) from the axial direction of the specimen and the azimuthal angle (0-360°) from a reference direction in the plane of the specimen. Pole figures were plotted with the compression axis (Z) at the centre and the transverse reference direction at the north pole. The azimuthal angle is measured in degrees, counterclockwise from the north pole, and the magnitude of the angle of tilt is proportional to the radial distance from the centre of the pole figure. Iso-intensity contours were plotted in units of multiples of the intensity of a random distribution of orientations (mrd). The pole figure data were employed to calculate crystal orientation distribution functions (CODF) using the series expansion method and the coefficients were then used to calculate inverse pole figures. The evolution of microstructure with deformation was followed using standard metallographic techniques.

RESULTS

Annealing Texture in Zr-2.5 Nb

Fig. 1 shows the (0002) and (10$\bar{1}$0) pole figures obtained after annealing at 1073 K. Similar results were obtained at 1123 K. The dual fibre texture of the as-received bar was 2-3 times sharper than in the as-received condition but its general characteristics remanined unchanged. This texture "memory" effect and the sharpening of the texture on (α+β)-annealing appears to be associated with the characteristics of the $\alpha \rightarrow (\alpha+\beta)$ transformation. On heating, recovery of the dislocation structure and α grain growth act to sharpen the texture by eliminating the spread of orientations within each grain. This enhances the growth of the <10$\bar{1}$0> and [0001] grain orientations at the expense of slightly misoriented grains. On cooling, the β phase transforms to α by growth of the pro-monotectoid α[2] and the characteristics of the original α texture are preserved.

Compression Texture in Fine Grained Zr-2.5 Nb

Figs. 2a and 2b illustrate the (0002) and (10$\bar{1}$0) pole figures, respectively, of the fine grained material deformed to ϵ=-0.20. The (10$\bar{1}$0) pole figure shows a maximum intensity at 30° from the compression axis. Thus, the grains initially rotate about their <c>-axis and, as a result, the main fibre changes to <11$\bar{2}$0> from its original <10$\bar{1}$0> form in the original bar. In addition, the maximum (0002) intensity observed at 90° from the specimen axis before annealing, is now located about 10° off the plane of the specimen. Thus, the grains that originally had <c>-axes at 90° from the compression axis also rotate so that their (0002) plane normals move slightly away from the plane of the specimen. The (0002) pole figure also shows that the [0001] fibre in the annealed material disappears after ϵ=-0.20, indicating

that the basal plane normals of these grains rotate away from the compression axis. Fig. 2c is an optical micrograph from the transverse section of a specimen deformed to ϵ=-0.40. Only isolated grains show evidence that mechanical twinning took place during deformation implying that most of the deformation was accommodated by slip. Fig. 3a shows the inverse pole figure for the compression axis of the specimen deformed to ϵ=-0.80. This inverse pole figure was calculated from the CODF coefficients. The texture is ill-defined and relatively weak with maximum intensities of about 3 mrd. It is clear that continued deformation has caused that the grains progressively rotate away from <10$\bar{1}$0> towards an orientation in which their basal plane normals are tilted about 15° from the compression axis within a spread of about 15°. The sharpness of the <11$\bar{2}$0> fibre formed at lower strains decreased to about half its value at ϵ=-0.20.

Compression Texture in Coarse Grained Zr-2.5 Nb

Figs. 4a and 4b show the (0002) and (10$\bar{1}$0) pole figures for the coarse grained specimen deformed to ϵ=-0.15. These pole figures are fundamentally different to those shown in Fig. 2 for the fine grained material. The [0001] fibre has now an intensity about 10 times as strong as in the annealed material. Concurrently, the <10$\bar{1}$0> fibre is about 6 times weaker than in the annealed sample. The increase in the sharpness of the [0001] fibre corresponds to the decrease in intensity of the initial <10$\bar{1}$0> fibre. Thus, the observed change in texture is consistent with a rapid 90° rotation of the (0001) plane normals about a <11$\bar{2}$0> direction. Fig. 4c shows an optical micrograph of the microstructure of a coarse grained specimen deformed to ϵ=-0.10. Twins, lenticular in shape, can be observed throughout the microstructure running across the α-Zr grains and stopping at grain or other twin boundaries.

DISCUSSION

Fig. 3b shows the predicted inverse pole figure for a collection of 160 orientations, initially regularly spaced in the unit triangle, after deformation to ϵ=-0.80 according to the full constraint model of texture evolution[3]. The simulation was carried out assuming that {10$\bar{1}$0}<1$\bar{2}$10>, (0002)<11$\bar{2}$0>, and {10$\bar{1}$1}<11$\bar{2}$3> slip systems were active with relative CRSS's of 0.1, 0.2 and 1.0, respectively. Comparison of Figs. 3a and 3b indicates that the model predicts qualitatively the reorientation tendencies observed experimentally. Thus, it appears that slip deformation is the controlling mechanism in fine grained material. This is most surprising since mechanical twinning is generally acknowledged to play a rate controlling role during deformation of hcp Zr[4].

The symmetry of the initial texture in the present material and the imposed strain path require accommodation of tensile strains parallel to the [0001] axes of the majority of the grains. All other strain components can be accounted

for by <a>-type slip (prismatic and/or basal). $\{10\bar{1}2\}\langle 10\bar{1}\bar{1}\rangle$ twins are formed when a tensile strain is imposed parallel to the <c>-axis of an α-Zr grain. When the twin is formed, its <c>-axis is related to the [0001] direction in the matrix by an 85° rotation about a $\langle 11\bar{2}0\rangle$ direction. This is entirely consistent with the compression texture developed in coarse grained Zr-2.5 Nb (Fig. 4).

The preceding discussion suggests that there is a competition between <c+a> slip and tensile twinning to control <c>-axis deformation. These two mechanisms require larger stresses to be activated than <a>-type slip[5]. Thus, generalized plastic flow and texture development will depend on the mode of <c>-axis deformation. The results of the present investigation suggest that the α grain size controls which mechanism is preferred for <c>-axis deformation.

Grain size affects the nucleation and growth of mechanical twins via the Hall-Petch relationship[6,7] with slip usually preceding the nucleation of twins[7]. Zircaloy-2 deformed in compression exhibits an elasto-plastic transition during which only prismatic slip is responsible for plastic flow[8]. <c+a> slip and twinning are not activated until plastic flow is fully established at total strains larger than -0.003. A similar behaviour was observed in the present coarse grained Zr-2.5 Nb specimens. The flow curve exhibited an elasto-plastic transition with a proportional limit of 280 MPa and a flow stress of 350 MPa at end of the transition. Fine grained specimens did not show an elasto-plastic transition and fully plastic flow was defined by a sharp yield point at 410 MPa. These observations suggest that the activation of <c+a> slip determines the onset of fully plastic deformation in fine grained Zr-2.5 Nb. In coarse grained material, the more extensive planar arrays of dislocations formed during the elasto-plastic transition[9] may have the effect of raising the local stress at points of stress concentration so that twins can be nucleated before <c+a> slip is activated. This effect may also be reinforced by the compatibility stresses developed to accommodate the mismatch between the α grains and the metastable β phase present in Zr-2.5 Nb. The reason why this should have a bigger effect in the coarse grained material remains still unclear. One further contribution to the preference of twinning in coarse grained material may be associated with a higher content of oxygen in solid solution due to the higher annealing temperature. This excess oxygen can lock up the <c+a> dislocations which would therefore require a higher activation stress allowing twinning to take place first. The occurrence of a sharp yield point in the fine grained material strongly supports this argument. The lattice reorientation associated with twinning requires <c+a> slip to accommodate further compressive deformation parallel to the <c>-axes of the twins. This causes an increasing work hardening rate as more material becomes reoriented with <c>-axes parallel to the compression axis. It was observed experimentally that the flow stress for fine and coarse grained Zr-2.5 Nb becomes equal at about ϵ=-0.15. This is consistent with the phenomenological model described above.

CONCLUSIONS

Texture evolution in Zr-2.5 Nb depends on the type of <c>-axis strain mechanism acting during deformation. The choice of mechanism is, in turn, determined by the size of the α-Zr grains. Tensile twinning is responsible for the formation of a sharp [0001] compression texture in coarse grained Zr-2.5 Nb. Slip deformation (prismatic, basal and <c+a> pyramidal) is responsible for the texture observed in fine grained Zr-2.5 Nb.

REFERENCES

1. C.E. Coleman, ASTM STP 754, D.G. Franklin, ed., ASTM, 1982, 393.
2. B.A. Cheadle an C.E. Ells, *Electrochem. Technol.*, **4**(1962)329.
3. A. Salinas R., Ph. D. Thesis, McGill University, 1988.
4. R.G. Ballinger, G.E. Lucas and R.M. Pelloux, *J. Nucl. Mater.*, **113**(1984)53.
5. A. Akhtar, J. Nucl. Mater., 47(1973)79.
6. M.J. Marcinkowski and H.A. Lipsitt, *Acta. Metall.*, **10**(1962)95.
7. D. Hull, *Acta Metall.*, **9**(1961)191.
8. S.R. MacEwen, N. Christodoulu, C. Tome, J. Jackman, T.M. Holden, J. Faber and R.L. Hitterman, ICOTOM-8 Conf. Proc., J.S. Kallend and G. Gottstein, Eds., TMS, 1988, 825.
9. S. Mahajan and D.F. Williams, *Inter. Metall. Revs.*, **18**(1973)43.

ACKNOWLEDGMENTS

The authors wish to recognize the technical assistance of J.F. Mecke and the helpful review of the manuscript by R. Holt and R. Ploc. The financial assistance of the CANDU Owners Group is also duly recognized.

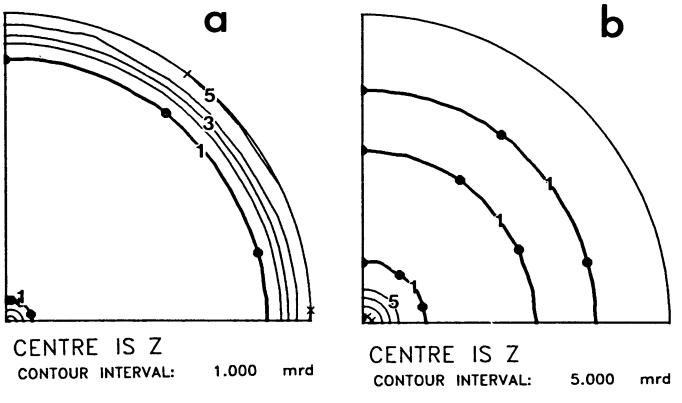

Fig. 1 (a) (0002) and (b) $(10\bar{1}0)$ pole figures for Zr-2.5 Nb ($\alpha+\beta$) annealed at 1073 K.

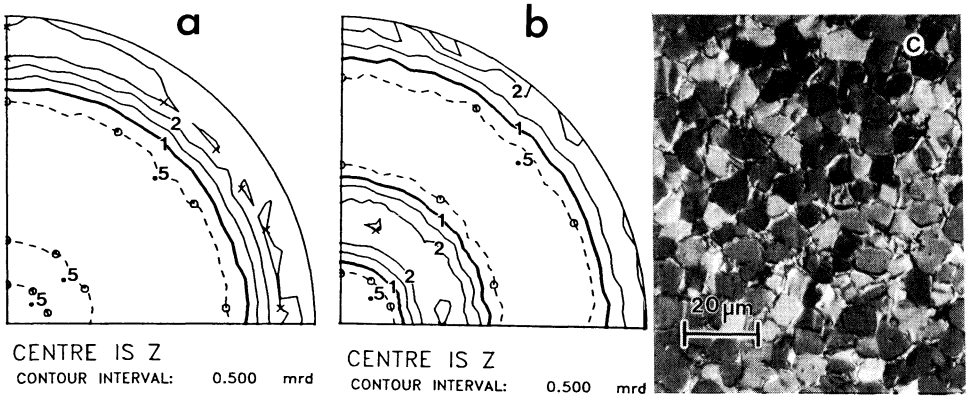

Fig. 2 (a) (0002) and (b) (10$\bar{1}$0) pole figures of Zr-2.5 Nb with an α grain size of 5 μm and deformed to ϵ=-0.20. (c) microstructure of a specimen deformed to ϵ=-0.40.

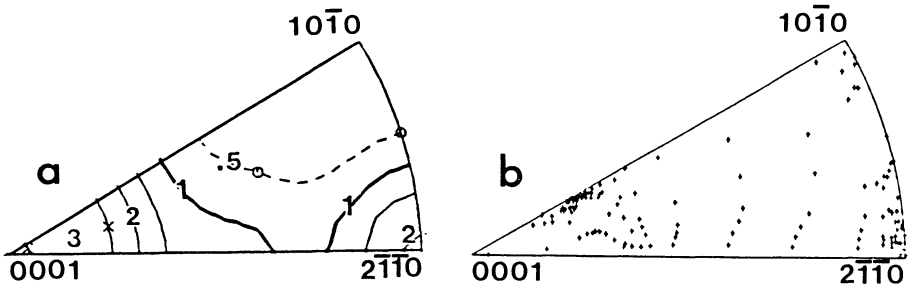

Fig. 3 Compression axis inverse pole figures for fine grained (5 μm) Zr-2.5 Nb deformed to ϵ=-0.80. (a) experimental, (b) predicted assuming full constraint deformation and <c+a> pyramidal, basal and prismatic slip.

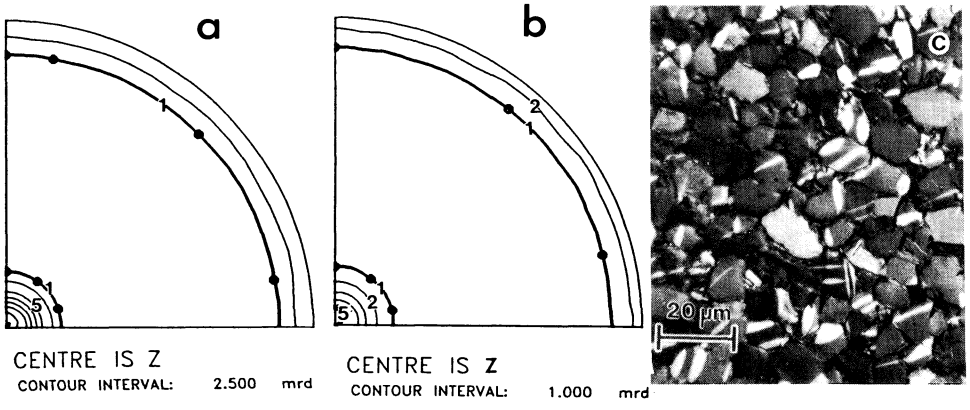

Fig. 4 (a) (0002) and (b) (10$\bar{1}$0) pole figures of Zr-2.5 Nb with an α grain size of 10 μm and deformed to ϵ=-0.15. (c) microstructure of a specimen deformed to ϵ=-0.10.